

Reversal-field memory in magnetic hysteresis

H. G. Katzgraber¹, F. Pázmándi¹, C. R. Pike², Kai Liu¹, R. T. Scalettar¹, K. L. Verosub², G. T. Zimányi¹

¹*Department of Physics, University of California, Davis, California 95616*

²*Department of Geology, University of California, Davis, California 95616*

(Dated: November 18, 2018)

We report results demonstrating a singularity in the hysteresis of magnetic materials, the reversal-field memory effect. This effect creates a nonanalyticity in the magnetization curves at a particular point related to the history of the sample. The microscopic origin of the effect is associated with a local spin-reversal symmetry of the underlying Hamiltonian. We show that the presence or absence of reversal-field memory distinguishes two widely studied models of spin glasses (random magnets).

PACS numbers: 75.50.Lk, 75.40.Mg, 05.50.+q

I. INTRODUCTION

Hysteresis is a widely observed phenomenon.¹ While many basic features are well understood^{2,3,4} a number of effects remain unresolved, such as the noise spectrum,⁵ frequency dependence,⁶ and exchange bias^{7,8} in the hysteresis of magnetic recording media.

Here we report a novel memory effect in magnetic systems that emerges when the magnetic field is first decreased from its saturation value and then increased again from some reversal field H_R . We find that the system exhibits a singularity at the negative of the reversal field, $-H_R$, in the form of a sharp kink in the magnetization. Microscopically a finite number of “symmetric clusters” are required for this effect to take place. In these clusters the central spins flip *after* all spins on the cluster boundary have flipped. In addition, the central spins experience zero effective local field so they are symmetric with respect to the change of direction of the external field. We have observed this “reversal-field memory” effect numerically in spin glasses, as well as experimentally in magnetic thin films commonly used in recording media.

To better illustrate the reversal-field memory effect we use the recently introduced first order reversal curve (FORC) diagram approach⁹ which captures the distribution of characteristic properties of hysteretic systems in great detail.

II. MODEL AND ALGORITHM

We study the Edwards–Anderson (EA) Ising spin-glass Hamiltonian¹⁰

$$\mathcal{H} = \sum_{\langle i,j \rangle} J_{ij} S_i S_j - H \sum_i S_i. \quad (1)$$

Here $S_i = \pm 1$ are Ising spins on a square lattice of size $N = L \times L$ in two dimensions with periodic boundary conditions. The exchange couplings J_{ij} are random nearest-neighbor interactions chosen according to a Gaussian distribution with zero mean and standard deviation unity, and H is the external magnetic field. The complex energy landscape of the EA spin glass will give rise to hysteretic behavior.

We simulate the zero temperature dynamics of the EA model by changing the external field H in small steps, first downward from positive saturation, and then upward from a reversal field H_R . After each field step, the effective local field h_i of each spin S_i is calculated:

$$h_i = \sum_j J_{ij} S_j - H. \quad (2)$$

A spin is unstable if $h_i S_i < 0$. We then flip a randomly chosen unstable spin and update the local fields at neighboring sites and repeat this procedure until all spins are stable.

III. RESULTS

Figure 1 shows a typical reversal curve. The area around $-H_R$ is enlarged in the inset and shows a sharp “kink”. The observation of any such sharp feature in a disordered system, especially of finite size and after disorder averaging, is quite remarkable.

The size of the change in slope can be characterized by measuring the slope of the magnetization curves to the left and right of $-H_R$, and comparing the difference with the average (see Fig. 2). The slope changes abruptly by as much as 30 % as we pass through $H = -H_R$. For this model, the range of reversal-field values for which the kink is present is roughly $-4.5 < H_R < -1.5$.

To develop an initial understanding of the microscopic origin of reversal-field memory, we first describe the conditions under which the effect occurs within the Preisach model.¹¹ In that approach, a magnetic system is described as a collection of independent two-state (± 1) switching units (“hystérons”). Unlike Ising spins, which always align with their local field, the hysteron’s state changes from -1 to $+1$ at a field $H_b + H_c$ different from the field $H_b - H_c$ required to switch the hysteron from $+1$ to -1 . Here H_b is the bias field and H_c is the coercivity of the hysteron. Different systems are then distinguished by their distribution $\rho(H_b, H_c)$ of hysterons of a given bias and coercivity, the so-called “Preisach function.”

For “symmetric hysterons,” i.e., $H_b = 0$, starting from a fully ‘up’ polarized state and decreasing the field to a negative H_R switches down all hysterons with $H_c < |H_R|$.

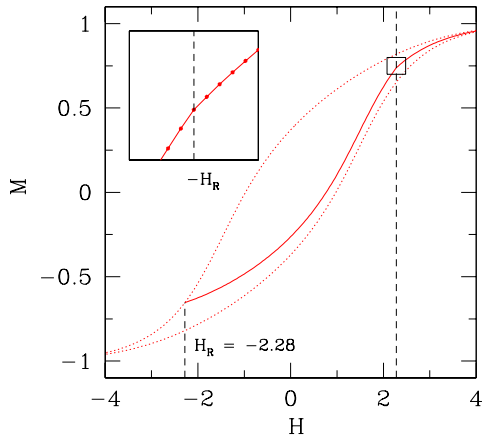


FIG. 1: Reversal-field memory effect: starting from positive saturation, the field is decreased to a negative reversal field H_R , then increased again. The inset shows the kink at $-H_R$. Data are from a two-dimensional EA Ising spin glass with 100^2 spins. The dotted line represents the major hysteresis loop, the dashed lines mark $\pm H_R$, respectively. In all figures the error bars are smaller than the symbols and the data are averaged over 1000 disorder realizations. In addition, H and M are in units of the interaction bond standard deviation, which in this work is set to unity.

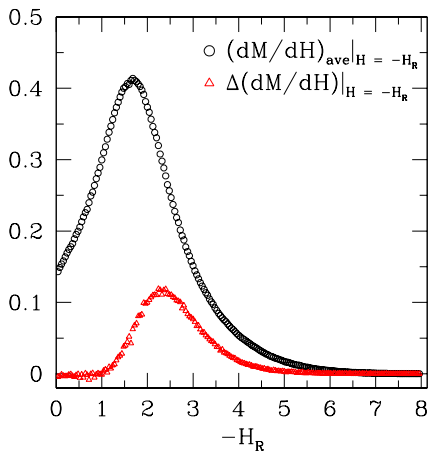


FIG. 2: The difference (triangles) and average (circles) of the left and right derivatives on either side of $-H_R$ for the EA Ising spin glass.

Reversing the direction of the sweep and increasing the field from H_R to $-H_R$ switches back every switched hysteron. Thus at $H = -H_R$ saturation is reached, creating a kink in the magnetization. Symmetric hysterons therefore give rise to reversal-field memory, but only if their number is macroscopic. In this case $\rho(H_b, H_c)$ must have a Dirac delta singularity at $H_b = 0$ and $H_c = |H_R|$. If the kink is observable in a range of H_R values, as in Fig. 2, then the singularities of the Preisach function form a ridge along the $H_b = 0$ axis for that range of H_c values.

The spins in the EA model are not independent. For

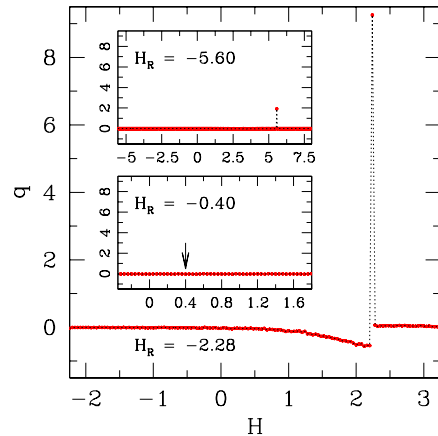


FIG. 3: Overlap function q of the spins flipping at H_R and at $H > H_R$, for $H_R = -2.28$. The insets show data for $H_R = -0.40$ and $H_R = -5.60$, respectively. The arrow in the inset marks $H = 0.40$.

them to behave as symmetric hysterons, they must possess a local spin-reversal symmetry. By local spin-reversal symmetry we mean that the local field h_i , felt by S_i [Eq. (2)], is perfectly reversed if the external field H is reversed and all spins coupled to S_i are reversed as well. In the EA Hamiltonian a cluster has this symmetry when all neighbors of S_i align with the local field before S_i does, both for decreasing and increasing fields, i.e., S_i flips down only after all of its neighbors are already negative, and during the reverse sweep S_i switches up only after all the neighbors.

The importance of the symmetric clusters can be appreciated by noticing that every spin of the EA model seems to have local spin-reversal symmetry. However, note that the spin configurations in general depend on the history of the sample in the glassy phase. Therefore, at $-H_R$ the neighbors of most spins do not necessarily point in a direction opposite of their direction at H_R , thus most EA spins do not belong to symmetric clusters. Hence the model Hamiltonian possessing a local spin-reversal symmetry is a necessary but not sufficient condition of having symmetric clusters. In order to test this conclusion we studied the random field Ising model (RFIM).^{2,10} In this model the couplings J_{ij} are chosen to be uniform, and the disorder is introduced through random local fields h_i . Direct inspection reveals that the RFIM does not possess a local spin-reversal symmetry, nor did we find a magnetization kink in our simulations.

To further illustrate the reversal-field memory effect, we define an overlap function q between the spins which flip at H_R and the spins which flip at $H > H_R$:

$$q(H) = \frac{1}{4} \sum_i [S_i(H_R + \delta) - S_i(H_R)] \times [S_i(H + \delta) - S_i(H)]. \quad (3)$$

Here δ is the field step. In Fig. 3 we show the overlap

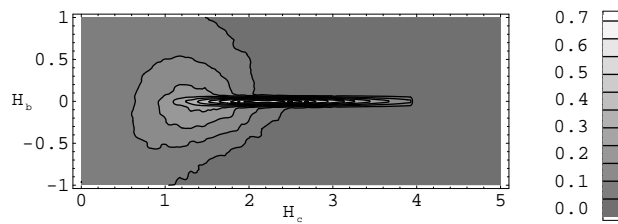


FIG. 4: FORC diagram of the EA Ising spin glass. Note the ridge along the H_c axis.

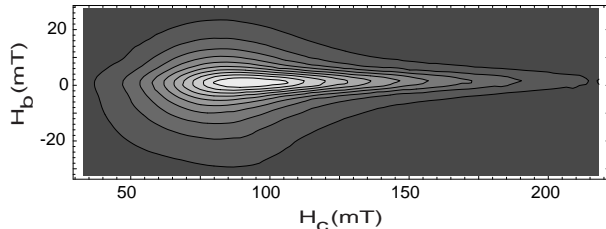


FIG. 5: Experimental FORC diagram of a Kodak sample. Note the similarity to the FORC diagram of the EA Ising spin glass shown in Fig. 4.

versus $H > H_R$ for $H_R = -2.28$. Clearly the spins which flip at H_R are highly correlated with the spins which flip at $-H_R$. This in turn shows that we have a macroscopic number of symmetric clusters. The insets show a much weaker effect at $H_R = -0.40$ and $H_R = -5.60$, values outside the ridge of Fig. 2.

The reversal-field memory can be characterized in greater detail by adapting a new tool developed for analyzing experimental data for hysteretic systems.⁹ In this method, a family of FORCs is generated by varying H_R in small steps. Let us denote by $M(H, H_R)$ the magnetization as the function of the applied and reversal fields. Computing the mixed second derivative with respect to H and the reversal field H_R yields the “FORC distribution” $\rho(H_c, H_b)$, where $H_c = (H - H_R)/2$ represents the local coercivity and $H_b = (H + H_R)/2$ the bias. FORC distributions are more general than Preisach distributions since they are model independent and allow for asymmetries and negative regions.

Figure 4 shows the FORC diagram of the EA model. The ridge along the H_c axis corresponds to the peak of Fig. 2 and is therefore a striking representation of the reversal-field memory effect. In contrast, the RFIM exhibits a vertical structure, even though both models have quite similar major hysteresis loops. This sensitivity of the FORC method makes it uniquely suited for analyzing details of hysteretic systems.

To demonstrate the existence of the reversal-field memory in magnetic media, in Fig. 5 we show an experimentally obtained FORC diagram of well-dispersed noninteracting single-domain magnetic Co- γ -Fe₂O₃ particles. Typically FORC diagrams of various systems exhibit extensive differences (see for example Ref. 12). There is a striking similarity between the experimentally and numerically determined FORC diagrams: both exhibit a narrow ridge along the H_c axis, the ridge “melting” with decreasing H_c and narrowing with increasing H_c . Simulations on more realistic systems with dipolar interactions, such as the ones found in the experimental sample, also show evidence of a ridge and therefore reversal-field memory.

IV. CONCLUSIONS

In conclusion, we report a reversal-field memory effect in disordered magnetic systems that manifests itself as a sharp kink in first order reversal curves, and as a sharp ridge on the zero bias axis of FORC diagrams. The effect has been observed numerically in the Edwards–Anderson Ising spin glass and experimentally in well-dispersed recording media samples. The origin of this effect is tied to a local spin-reversal symmetry, and has its microscopic origin in the development of a macroscopic density of symmetric clusters. Our studies also establish that the FORC method is a powerful diagnostic tool for characterizing magnetic materials.

V. ACKNOWLEDGMENTS

This work was supported by NSF Grant Nos. DMR-9985978, 99-09468, and INT-9720440.

- ¹ G. Bertotti, *Hysteresis and Magnetism for Physicists, Materials Scientists, and Engineers* (Academic Press, New York, 1998).
- ² J. P. Sethna, K. Dahmen, S. Kartha, J. A. Krumhansl, B. W. Roberts, and J. D. Shore, Phys. Rev. Lett. **70**, 3347 (1993).
- ³ I. F. Lyuksyutov, T. Nattermann, and V. Pokrovsky, Phys. Rev. B **59**, 4260 (1999).
- ⁴ J. Zhu, in *Magnetic Recording Technology*, edited by C. D. Mee and E. D. Daniel (Mc Graw Hill, New York, 1990).
- ⁵ H. N. Bertram, *Theory of Magnetic Recording* (Cambridge University Press, Cambridge, U.K., 1994).
- ⁶ M. Lederman, S. Schultz, and M. Ozaki, Phys. Rev. Lett.

- 73**, 1986 (1994).
- ⁷ W. H. Meiklejohn and C. P. Bean, Phys. Rev. **105**, 904 (1957).
- ⁸ J. Nogués and I. K. Schuller, J. Magn. Magn. Mater. **192**, 203 (1999), (recent review).
- ⁹ C. R. Pike, A. P. Roberts, and K. L. Verosub, J. Appl. Phys. **85**, 6660 (1999).
- ¹⁰ K. Binder and A. P. Young, Rev. Mod. Phys. **58**, 801 (1986).
- ¹¹ F. Preisach, Z. Phys. **94**, 277 (1935).
- ¹² C. R. Pike, A. P. Roberts, M. J. Dekkers, and K. L. Verosub, Phys. Earth Planet. Inter. **126**, 11 (2001).